Neurotoxicology 74 (2019) 252–263

Contents lists available at ScienceDirect

Neurotoxicology

journal homepage: www.elsevier.com/locate/neuro

Full Length Article

Neuroprotection by luteolin and gallic acid against cobalt chloride-induced behavioural, morphological and neurochemical alterations in Wistar rats

A.S. Akinrinde*, O.E. Adebiyi

Department of Veterinary Physiology and Biochemistry, Faculty of Veterinary Medicine, University of Ibadan, Nigeria

ARTICLE INFO

Keywords:
Cobalt
Neurotoxicity
Purkinje cells
Oxidative stress
Acetylcholinesterase

ABSTRACT

Cobalt (Co) intoxication arising from occupational exposures and ion release from metal implants has been associated with neurological alterations such as cognitive decline, incoordination and depression. The present study evaluated the mechanisms of neuro-protection exerted by Luteolin (Lut; 100 mg/kg) and Gallic acid (GA; 120 mg/kg) in Wistar rats exposed to cobalt chloride ($CoCl_2$) at 150 mg/kg for 7 consecutive days. Results indicate that $CoCl_2$ induced neuro-behavioural deficits specifically by decreasing exploratory activities of $CoCl_2$-exposed rats, increased anxiety, as well as significant reduction in hanging latency. Co-treatment with Lut or GA, however, restored these parameters to values near those of normal controls. Moreover, Lut and GA prevented $CoCl_2$-induced increases in hydrogen peroxide (H_2O_2), malondialdehyde (MDA) and nitric oxide (NO) in the brain, while also restoring the activities of acetylcholinesterase, glutathione S-transferase (GST) and superoxide dismutase (SOD). In addition, Lut and GA produced significant reversal of $CoCl_2$-induced elevation in levels of serum Interleukin 1 beta (IL-1β) and Tumor necrosis factor (TNFα). Meanwhile, immunohistochemistry revealed increased astrocytic expression of glial fibrillary acidic protein (GFAP), with intense calbindin (CB) D-28k staining and pronounced dendrites in the Purkinje cells. In contrast, the $CoCl_2$ group was characterized by decreased number of neurons expressing CB and dendritic loss. Taken together, mechanisms of luteolin and/or gallic acid protection against Co toxicity involved restoration of Ca^{2+} homeostasis, acetylcholinesterase and antioxidant enzyme activities, as well as inhibition of lipid peroxidation in the brain.

1. Introduction

Heavy metals are now increasingly implicated in the multi-factorial aetiology of many neurological disorders. Cobalt (Co), in living tissues, occurs most abundantly in association with Vitamin B12 (cobalamin). Deficiencies of this metal manifests in disorders including pernicious anaemia, slow growth rate, digestive disorders and myelin sheath damage (Olivieri et al., 2001). On the other hand, high levels of cobalt occur in the earth crust with potential exposures of humans and animals to high concentrations of the metal in contaminated food and water (Cheyns et al., 2014). Symptoms of Co toxicity have also been described following occupational exposure, as well as after consumption of large quantities of cobalt-containing supplements, foods and drinks (Tvermoes et al., 2013). Over-medication and illegal doping of human athletes and racehorses with cobalt-containing compounds have also been described (Mobasheri and Proudman, 2015).

Co is increasingly used as an orthopaedic metal (e.g. in metal-to-metal hip protheses), although its use has recently come under criticisms due to associated neurological disorders such as tremors, incoordination, cognitive decline, depression, hearing loss and visual changes in patients (Keegan et al., 2019; Mao et al., 2011). *In-vitro* evidences of Co-induced neurotoxicity have also been reported, including induction of β amyloid (Aβ) release in SHSY5Y neuroblastoma cells (Olivieri et al., 2001) and in $CoCl_2$-induced cytotoxicity in PC-12 cells (Jiang et al., 2017).

Co is a potent hypoxia-inducing agent, acting via mechanisms that stabilize the hypoxia-inducible factor alpha (HIFα), a protein that has been associated with an over-stimulation of the pro-death response, manifesting in cell injury and apoptosis. To achieve this, Co inhibits the hydroxylation of HIFα by prolyl hydroxylases, a process that normally targets the protein for degradation (Vengellur and LaPres, 2004; Mohamed et al., 2019). Co toxicity is also associated with an over-production of reactive oxygen species and induction of oxidative stress (Tan et al., 2009; Kubrak et al., 2011). Hypoxia and oxidative stress play important roles in the pathogenesis of neuronal disorders and neurodegenerative diseases (Jiang et al., 2017). Exposure to high concentrations of Co thus has high potential to mediate cell cytotoxicity, as well as metabolic disturbances in sensitive cells such as neurones.

* Corresponding author.
E-mail address: as.akinrinde@gmail.com (A.S. Akinrinde).

https://doi.org/10.1016/j.neuro.2019.07.005
Received 22 April 2019; Received in revised form 20 July 2019; Accepted 21 July 2019
Available online 27 July 2019
0161-813X/

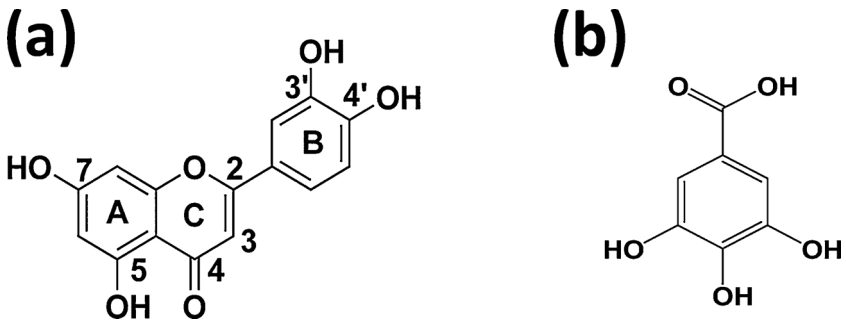

Fig. 1. Structures of (a) Luteolin and (b) Gallic acid.

Crucially, it was recently shown that both $CoCl_2$ and cobalt nanoparticles (CoNPs) exerted adverse effects on neurons with the latter showing greater neurotoxicity (Zheng et al., 2019).

Luteolin (3′,4′,5,7-tetrahydroxyflavone) is a naturally-occurring flavonoid is found in many fruits, vegetables and medicinal plants (Lin et al., 2008). Biologically, it functions as an antioxidant, anti-inflammatory and anticancer agent. The hydroxyl groups present at carbons at positions 5, 7, 3′ and 4′ in the flavonoid structure are structurally important features that are associated with these biological activities (Fig. 1a). Luteolin, like most flavonoids is rapidly and efficiently absorbed in the intestine. It, however, undergoes extensive metabolism to different metabolites or conjugates (e.g. luteolin-3′-*O*-β-d-glucuronide) which causes the bioavailability of the unchanged luteolin to be relatively low. Studies have, however, suggested that the metabolites or conjugates may account for a large portion of the bioactivities of this flavonoid (Deng et al., 2017). Luteolin's cellular protection against oxidative stress is believed to arise from its direct free radical scavenging activities, while it also acts indirectly by modulating the pathway(s) involved in expression of cytoprotective enzymes and molecules, including the inducible Keap1-Nrf2-ARE pathway which coordinates the expression of phase II detoxifying and antioxidant enzymes such as glutathione S-transferase (GSTs) (Zhang et al., 2013).

In this study, we investigated possible mechanisms of Co toxicity in the nervous system by examining its effects on neurobehavioral parameters, oxidative stress, inflammation, as well as some key protein indicators of injury in the brain of rats. Furthermore, we examined the neuro-protective effects of luteolin on the above parameters. We have previously explored the protective effects of Gallic acid (Fig. 1b) against Co-induced toxicities in cardiac and renal tissues (Akinrinde et al., 2016a, 2016b). However, its neuro-protective potential against Co-induced toxicity in nervous tissues is yet to be investigated. Gallic acid is a well known phenolic antioxidant considered as an excellent free radical scavenger. It has previously been shown to exert neuroprotective activity against 6-hydrohydopamine-induced oxidative stress via enhancement of rat cerebral antioxidant defence (Mansouri et al., 2013). Gallic acid was thus investigated alongside luteolin, as a standard neuroprotective antioxidant, in the present study.

2. Materials and methods

2.1. Chemicals and kits

Cobalt chloride hexahydrate ($CoCl_2{\cdot}6H_2O$) was obtained from Tianjin Kermel Chemical Reagent Co., China. TNF-α and IL-1β ELISA kits were obtained from Elabscience®, United Kingdom. Luteolin, gallic acid, glutathione, 1, 2-dichloro-4-nitrobenzene (CDNB), thiobarbituric acid (TBA), trichloroacetic acid (TCA), sodium hydroxide, xylenol orange, potassium hydroxide, and hydrogen peroxide were purchased from Sigma–Aldrich (St. Louis, Missouri, USA). All other chemicals were of the highest purity commercially available.

2.2. Animals and experimental design

Forty eight male Wistar rats, about 8 weeks old and weighing about 100 ± 20 g used in this study were obtained from the Experimental Animal Unit, Faculty of Veterinary Medicine, University of Ibadan, Nigeria. They were housed in plastic cages in a well-ventilated animal house with natural photoperiod of 12-hr light and 12-hr dark, and were provided throughout the study period with standard rat chow plus water *ad libitum*. The protocols for handling of the rats were according to guidelines stated in the 'Guide for the Care and Use of Laboratory Animals' prepared by the National Academy of Science (NAS) and published by the National Institute of Health (NIH Publication No. 85–23, revised 1996 (PHS, 1996) and was approved by the Animal Care and Use Research Ethics Committee of the University of Ibadan

The animals were randomly assigned to four groups of 12 rats each and were treated as follows:

Group A: Control rats (given distilled water by oral gavage).

Group B ($CoCl_2$): Rats exposed to Cobalt chloride ($CoCl_2$) at 150 mg/kg by oral gavage for 7 consecutive days.

Group C ($CoCl_2$ + Lut): Rats treated with Cobalt chloride ($CoCl_2$) at 150 mg/kg plus Luteolin (Lut) at 100 mg/kg orally for 7 consecutive days.

Group D ($CoCl_2$ + GA): Rats treated with Cobalt chloride ($CoCl_2$) at 150 mg/kg plus Gallic acid (GA) at 120 mg/kg orally for 7 days.

The doses of $CoCl_2$ (Speijers et al., 1982; Awoyemi et al., 2017), Luteolin (Lu et al., 2015; Oyagbemi et al., 2018) and Gallic acid (Akinrinde et al., 2016b) were chosen based on previous relevant publications.

2.3. Behavioural tests

Following exposure to the different compounds, different neurobehavioural tests were carried out to assess learning, memory, motor co-ordination, locomotor activity and anxiety in the rats

2.3.1. Hanging wire tests

On day 6, the rats were suspended on to a single wire (2 mm in diameter, 100 cm in length) stretched between two posts 50 cm above the ground. The rats were made to grasp the wire with their forelimbs; to prevent the animal from using all four paws, the hind limbs were gently covered with adhesive tape. A pillow was placed between the two posts to avoid injury when the rats fall. 'Latency to fall' is the primary end point used to assess motor performance. The latency to fall was recorded with the aid of a stopwatch by an observer blinded to the treatment groups. The cut off was 120 s per animal (Aartsma-Rus and van Putten, 2014). The test was repeated for each rat after a 2-hr rest period.

2.3.2. Morris water maze

The water maze was used as previously described (Zhao et al., 2008). The maze was a circular tank 100 cm in diameter, 30 cm deep, filled with water (26 ± 1 °C) to a depth of 25 cm and divided into four

quadrants. A transparent round platform (escape platform) 10 cm in diameter was placed at 0.5 cm below the surface of the water one quadrant of the pool. The water was made opaque with non-fat milk. The latency to find platform was recorded with the aid of a stopwatch by an observer blinded to the treatment groups.

During the acquisition (short term or spatial memory) trial, each rat underwent four trials (different starting positions located 90° apart on the perimeter of the pool) per day for 4 days (days 4–8). During the test of spatial memory, the animals learnt to use distinctive visual cues surrounding the pool to navigate a direct path to the escape platform. The platform remained in a constant location during the acquisition phase. Animals were placed on the platform 30 s preceding the start of each training session. Each rat was then gently immersed in the water at one of the four randomized start locations and allowed 120 s to escape onto the platform. If the rat failed to escape within this time, it was guided to the platform. Once the rat reached the platform, it remained there for 15 s. The rat was returned to its home cage between trials. The learning curve for each animal was constructed by plotting the trial number on x-axis and latency to find platform in seconds on y-axis (Morris, 1984; Li et al., 2008).

The probe trial (working memory) was performed 24 h after the last acquisition trial, in which the platform was removed. Performance (the number of crossings over the position at which the platform had been located and the swimming time in the quadrant of the former platform position) were recorded according to Golchin et al. (2013). Briefly, data for the probe trail was collected with a digital camera (ICD-49 B/W camera, Ikegami Tsushinki Company, Ltd, Japan) of 1280 × 1024 pixels resolution mounted above the maze. During recordings, the camera recorded digital video to a computer equipped with iSpy (an open source animal behavior tracking software) dedicated behavioral analysis software. All behavioral analyses were thereafter performed from the video by an observer blinded to the treatment conditions.

2.3.3. Open field test

The general exploratory activity was measured on day 7 in an open field box. The rats were placed at the centre of the box and tested for 5 min. The apparatus was constructed with white plywood and measured 72 cm (L) × 72 cm (W) cm × 36 cm (H). One of the walls was made with plexiglass so rats could be visible in the apparatus. Black lines were drawn on the floor with a marker; the lines divided the floor into sixteen 18 × 18 cm squares. A central square (18 cm × 18 cm) was drawn in the middle of the open field. The open field maze was cleaned between each rat using 70% ethyl alcohol. A digital camera (ICD-49 B/W camera, Ikegami Tsushinki Company, Ltd, Japan) of 1280 × 1024 pixels resolution was mounted on a stand so that each rat could always be visualized from above while in the Open field test arena. During recordings, the camera recorded digital video to a nearby computer equipped with iSpy (an open source animal behavior tracking software) dedicated behavioral analysis software. All behavioral analyses were thereafter scored from the video by an observer blinded to the treatment conditions. At the beginning of the session, each rat was placed in the centre of the box. Frequency of grid crossing, rearing, stretch-attend posture, number of faecal boli, centre square and freezing durations were scored as described by Brown et al. (1999). Briefly, the frequency of grid crossing is the number of times a rat crossed from one square to another entering with at least its two front paws. Rearing is the number of times rat stood on its hind legs. Stretch attend Posture is the frequency with which the rat demonstrated forward elongation of the head and shoulders followed by retraction to the original position. Faecal boli represents the number of fecal boli deposit or defecation. Centre square duration is the period spent within the centre of the test box. Freezing represents the duration at which the rat was completely stationary and immobile. At the end of each session, rats were removed from the open field and the experimental box was thoroughly cleaned with 50% alcohol and dried between subjects in order to avoid olfactory cuing (Varga et al., 2015).

2.4. Animal sacrifice and tissue preparation

Following the performance of all behavioural tests, blood samples were collected from eight rats in each group via the retro-orbital plexus into plain sample bottles. The blood was allowed to coagulate for at least 1 h and was later centrifuged at 3000 rpm for 5 min to separate the serum, which were stored in Eppendorf tubes and frozen at −20 °C till use. The rats were then sacrificed by cervical dislocation, following which the brain was isolated and rinsed in in 1.15% KCl. Whole brain samples from five rats were homogenized in 50 mM Tris–HCl buffer (pH 7.4) containing 1.15% potassium chloride, and were later centrifuged at 12,000 x g for 10 min at 4 °C using a cold centrifuge. The supernatant collected was used for the determination of biochemical parameters.

For immunohistochemistry, four rats per group were deeply anesthetized with an intraperitoneal injection of sodium pentobarbital (25 µg/10 g body weight) and were perfused with 0.9% NaCl followed by 4% paraformaldehyde in 0.1 M phosphate buffer, pH 7.4. The brains were immersed in the same fixative, embedded in paraffin and sectioned serially in the mid-sagittal plane at 4 µm.

2.5. Biochemical assays

Protein concentration was measured by the Biuret method as described by Gornal et al. (1949). Nitric oxide (NO) level in the brain tissues was measured as the content of nitrites, according to the method described by Olaleye et al. (2007). The nitrite content was obtained using a sodium nitrite curve as standard and expressed as µmol of nitrites/litre. Hydrogen peroxide (H_2O_2) concentration was determined spectrophotometrically at 560 nm using the method of Wolff (1994). Malondialdehyde (MDA) concentration as an index of lipid peroxidation was estimated using the method of Varshney and Kale (1990). MDA content was quantified with a molar extinction coefficient of $1.56 \times 105 M^{-1} cm^{-1}$ and expressed as micromoles per gram of tissue. Tissue content of reduced glutathione (GSH) was measured by the method of Beutler et al. (1963). Superoxide dismutase (SOD) activity was determined according to the method described by Misra and Fridovich (1972) with slight modifications by Oyagbemi et al. (2015). The assay is based on the inhibition of the auto-oxidation of epinephrine at pH 7.2 at 30 °C. Briefly, 100 mg of epinephrine was dissolved in 100 mL distilled water and acidified with 0.5 mL concentrated hydrochloric acid. Then, 0.01 mL of each sample was added to 2.5 mL of 0.05 mol/L carbonate buffer (pH 10.2), followed by the addition of 0.3 mL of 0.3 mmol/L epinephrine. The increase in absorbance at 480 nm was monitored every 30 s for 150 s. One unit of SOD activity represents the amount of SOD necessary to cause 50% inhibition of the oxidation of adrenaline to adrenochrome during 1 min. Glutathione-*S*-transferase (GST) activity was estimated by the method of Habig et al. (1974) using 1-chloro-2, 4-dinitrobenzene (CDNB) as substrate. Glutathione peroxidase (GPx) activity was determined using the method of Rotruck et al. (1973).

2.6. Determination of serum levels of pro-inflammatory cytokines

Serum concentrations of Interleukin 1 beta (IL-1β) and Tumor Necrosis Factor alpha (TNF-α) were determined using commercially available enzyme linked immuno-sorbent assay (ELISA) kits (Elabscience®, UK) according to the manufacturer's instructions.

2.7. Immunohistochemistry

The tissues were dehydrated, embedded in paraffin, and sectioned into 5 µm sections. The sections were deparaffinized with xylene, rehydrated with alcohol and washed with phosphate buffered saline (PBS) for 5 min. Antigen retrieval was done in 10 mM citrate buffer (pH = 6.0) for 15 min at 96 °C, with subsequent peroxidase quenching in 3% H_2O_2/methanol. All the sections were blocked in 2% milk for 1 h

and probed with the following antibodies overnight: anti-GFAP Rabbit Polyclonal antibody for astrocytic morphology (1:1000; Z0334, Agilent Technologies®, USA) and anticalbindin (D-28k) rabbit monoclonal antibody (1:12000; CB-38, Swamy®, Switzerland) for Purkinje cells and dendrites morphology for 16 h at 4 °C. After washing, the sections were incubated for 2 h at room temperature and exposed to secondary antibody (goat anti-rabbit IgG, diluted 1:200; Vector Labs). The sections were then reacted in avidin-biotin-peroxidase solution (ABC kit, Vectastain, Vector Labs, USA) using 3, 30-diaminobenzidine (DAB) as chromogen and counterstained with hematoxylin (Rajabzadeh et al., 2012; Jalayeri-Darbandi et al., 2018) according to manufacturer's protocol. Images were acquired with digital microscope (Leica DM 750 HD& IC50 E, Leica microsystem®).

2.8. Quantification of cell numbers

The astrocytes were counted using imageJ® software. Briefly, the cell of interest was identified in the investigated brain region, plugins were then used to analyse and count the cells as described (Jensen, 2013). Cell numbers were expressed per mm^2.

The total number of Purkinje cells was counted by scanning the entire length of the Purkinje cell layer. Purkinje cells were identified based on Calbindin positivity and their specific location. To account for the difference in section sizes and plane of cutting, the length of the Purkinje cell layer was traced and measured in each section using ImageJ® software to obtain the number of Purkinje cells per standardized unit length (mm). For these sections, the length of Purkinje cell layer was measured and the number of Purkinje cells in each area counted.

2.9. Statistical analysis

Statistical analysis was performed using the GraphPad Prism software (Version 7.00). Results of behavioural tests and biochemical analyses were expressed as mean ± standard deviation and analysed using one way Analysis of Variance (ANOVA). P-values < 0.05 were considered statistically significant. The open field, hanging wire and the probe trial of the Morris water maze task results were analyzed by one-way analysis of variance (ANOVA) followed by the Tukey's post hoc test for multiple comparisons. Group differences in the escape latency of the acquisition trial in the Morris Water Maze test were analyzed using two-way ANOVA with repeated measures followed by Tukey's post hoc test.

3. Results

3.1. Hanging wire

The results of the hanging wire test on day 8 showed that there was a significant decrease in the mean time spent by the rats in hanging wire in the cobalt chloride ($CoCl_2$) group compared with the control ($P < 0.05$). Co-treatment with luteolin or gallic acid, however, produced significant increase ($P < 0.01$) in the hanging latency when compared with the $CoCl_2$ group (Fig. 2).

3.2. Morris water maze

The spatial learning and memory in the different groups were assessed by the Morris water maze test. The escape latency for finding the hidden platform is depicted in (Fig. 3). Across the groups, rats showed a marked reduction in escape latencies from day 1 to day 4 of the trial. In addition, the control and $CoCl_2$ + luteolin exhibited significant differences in escape latencies on day 2 when compared with the other groups (Fig. 3a). Furthermore, the escape latencies significantly reduced with increase in number of trials in all the groups (Fig. 3a).

As illustrated in Fig. 3b there were no significant differences in percent of total time spent in target quarter of the maze during the probe trial amongst all the groups.

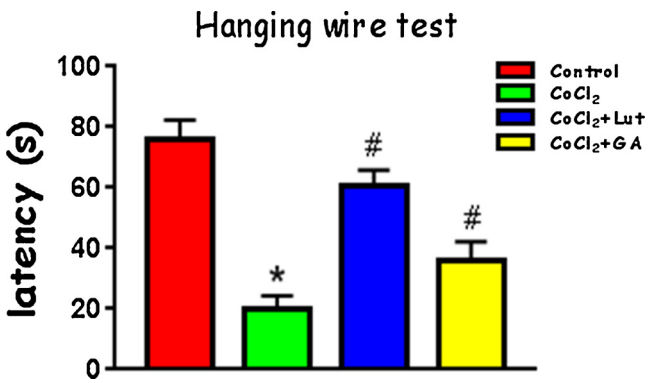

Fig. 2. Hanging latency on the hanging wire test.
* Significantly different from control, # significantly different from cobalt only group

3.3. Open field test

The open field test was conducted to examine locomotor activity and anxiety-related behaviour. This study showed significant differences in the effects of $CoCl_2$ treatment in contrast with the control and luteolin-treated groups. Significant differences were noticed in the rearing frequency, freezing duration, stretched-attend posture, time spent in centre and number of faecal boli between the $CoCl_2$ and the treated groups (Fig. 4). The grid crosses were significantly decreased ($p < 0.05$) in $CoCl_2$ treated groups compared to other groups (Fig. 4A). Similarly, the rearing frequency was decreased ($P < 0.05$) in $CoCl_2$ treated groups compared to luteolin-treated rats (Fig. 4B). The number of faecal boli and freezing duration was significantly increased ($P < 0.05$) in $CoCl_2$-treated groups in comparison with control and $CoCl_2$ + luteolin groups, while the stretched attend posture in the $CoCl_2$ group was significantly higher ($P < 0.05$) than those of control rats (Fig. 4 C–E). Furthermore, rats in the $CoCl_2$ group spent more time in the centre of the box in comparison to those in the other groups (Fig. 4F). As shown in Fig. 4 A–F, the effects of luteolin on $CoCl_2$-induced neuro-behavioural changes, as explained above, were largely similar to those produced by gallic acid.

3.4. Brain oxidant-antioxidant status

Oxidative changes induced by $CoCl_2$ were assessed by measuring markers of oxidative stress, including Nitric oxide (NO), Hydrogen peroxide (H_2O_2), malondialdehyde (MDA) and reduced glutathione (GSH) levels (Fig. 5 A–D). The results indicate that $CoCl_2$ administration produced significant increases ($P < 0.05$) in brain levels of NO, MDA and H_2O_2 along with reduction in levels of GSH, when compared to the control rats. In contrast, co-administration with luteolin or gallic acid caused significant reductions in NO, MDA and H_2O_2, when these were compared with rats exposed to $CoCl_2$ alone. Levels of GSH were, however, not markedly altered by luteolin or gallic acid administration compared to the other groups of rats.

Further evidence of oxidative changes was indicated by changes in the activities of antioxidant enzymes, glutathione peroxidise (GPx), superoxide dismutase (SOD) and glutathione S-transferase (GST) (Fig. 6 A–C). CoCl2 administration produced significant reduction ($P < 0.05$) in GPx and SOD activities (Fig. 6 A and B), when compared with the controls, without altering the activity of GST (Fig. 6 C). Co-administration of $CoCl_2$ with Luteolin, however, resulted in significant enhancement of SOD and GST activities, when compared with the rats treated with $CoCl_2$ alone.

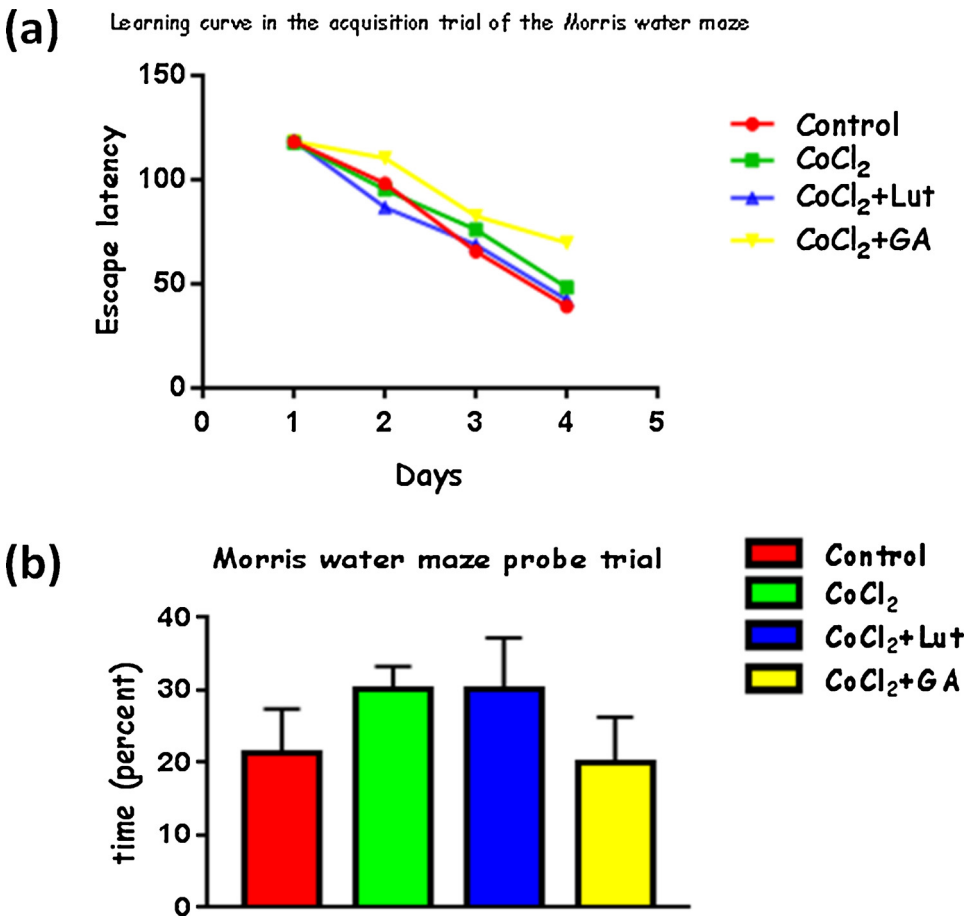

Fig. 3. Effect of cobalt on spatial learning and memory in the Morris water maze. a. Escape latency in the acquisition trial of the Morris water maze **b**. Mean percentage of total time spent swimming in the target quadrant in the probe trial of Morris water maze.

3.5. Serum inflammatory cytokines

Administration of $CoCl_2$ alone produced marked elevation ($P < 0.05$) in the serum levels of pro-inflammatory cytokines, Interleukin 1 beta (IL-1β) and tumour necrosis factor alpha (TNF α), when compared with the control (Fig. 7A and B). However, administration of rats with either Luteolin or Gallic acid caused significant restoration of the levels of these cytokines to control levels.

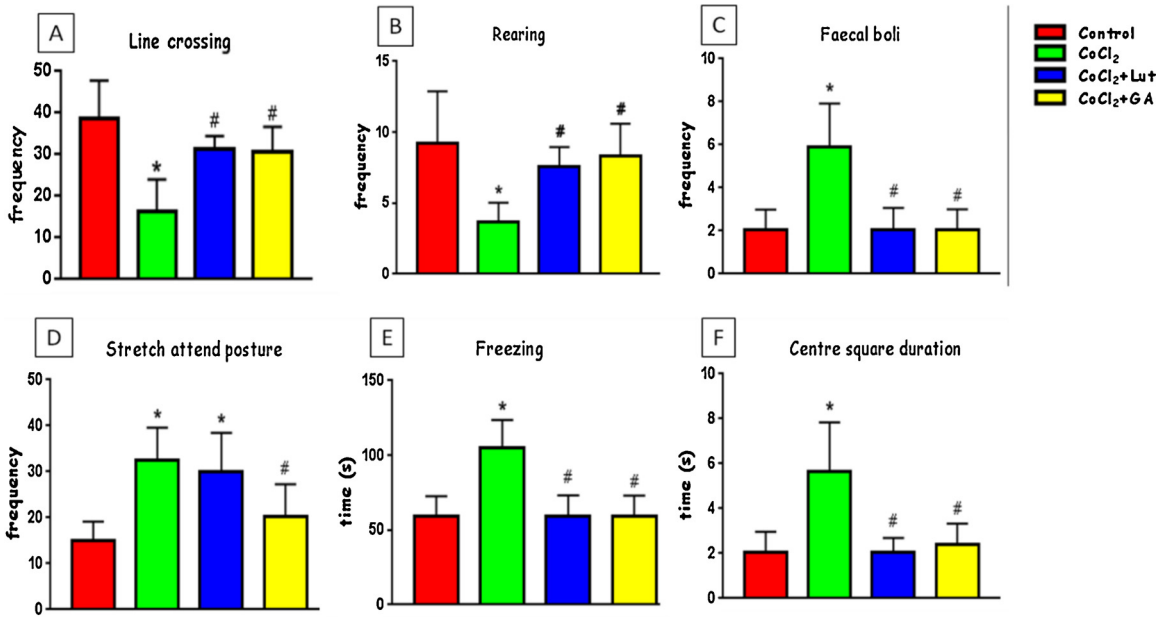

Fig. 4. Number of line crossings and rearing, faecal boli, stretch attend posture, centre square duration and freezing time in the open field test.
* Significantly different from control, # significantly different from $CoCl_2$ only group.

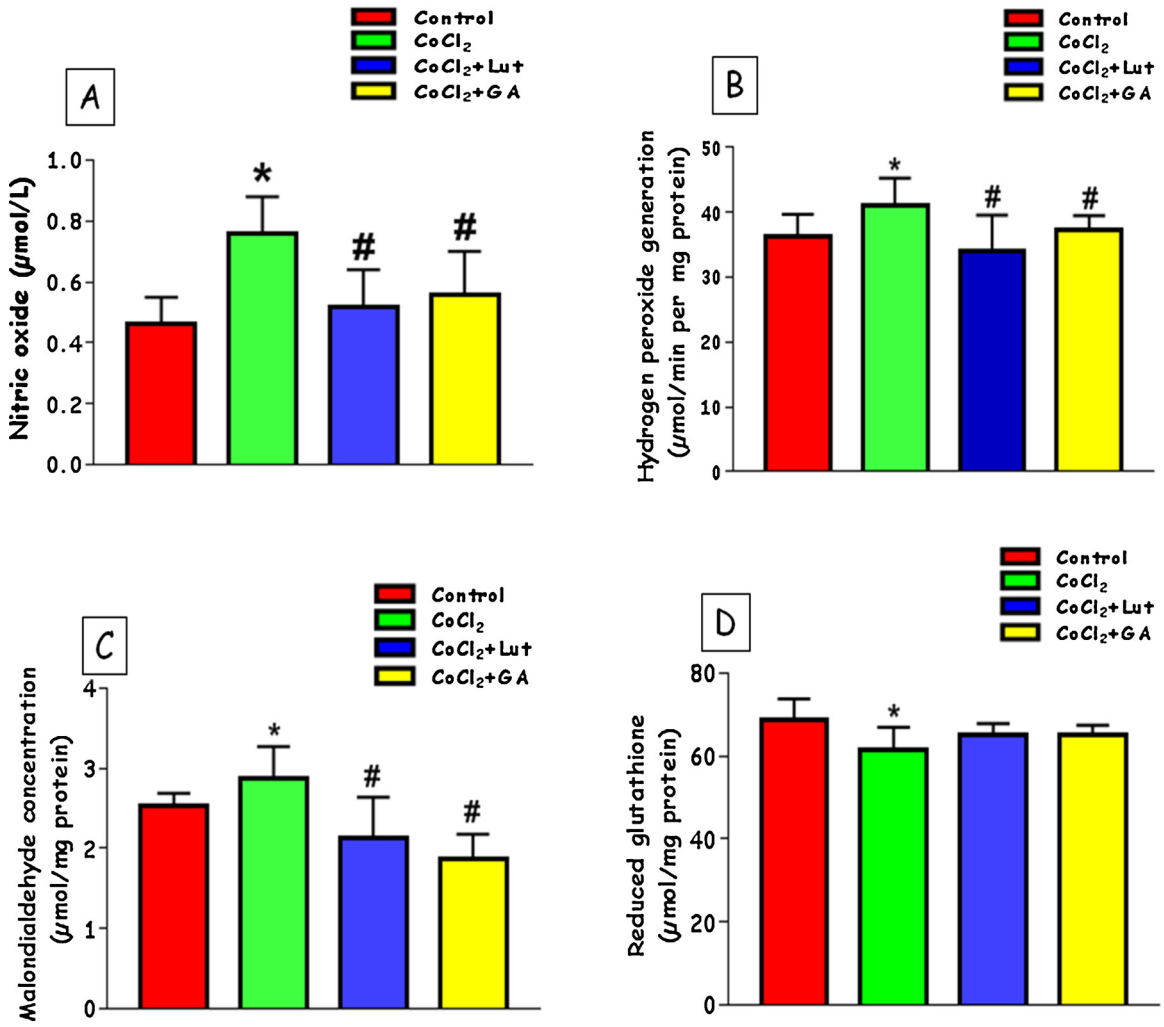

Fig. 5. Effect of Luteolin and Gallic acid on oxidative/nitrosative stress parameters in brain of rats exposed to Cobalt chloride. Values are expressed as mean ± standard deviation. * Significantly different from control, # significantly different from $CoCl_2$ only group.

3.6. Immunohistochemistry

Evaluation of samples prepared for the immunohistochemistry techniques showed that GFAP-positive cells were visible in the cerebellum of the different groups, although the numbers of these glial cells were highest in the $CoCl_2$group, lesser in the $CoCl_2$ + luteolin group and $CoCl_2$ + gallic groups and least in the control groups (Fig. 8 A–D). The morphological appearance of astrocytes revealed only thin cells with few short processes in the control rats (Fig. 8E). However, after $CoCl_2$ administration, astrocytes became multipolar and hypertrophic (Fig. 8F). All these effects were similarly observed in rats co-administered with luteolin and gallic acid (Fig. 8G-H). Quantitative count also revealed the expression of GFAP was highest in the $CoCl_2$ rats.

Calbindin immunoreactivity was used to identify Purkinje cells within cerebellar tissue. Purkinje cells were readily identified based on their unique morphology and location; their perikaryon situated within the Purkinje cell layer positioned between the granular cell and molecular layers across all the groups (Fig. 9A–D). However, a significant reduction in the number of Purkinje cells was observed in the $CoCl_2$ and $CoCl_2$ + gallic groups. The few calbindin-positive Purkinje cells seen in these groups displayed axonal loss with disorganized cell bodies (Fig. 9B, D, G, H). In contrast, Purkinje cells in the control and $CoCl_2$ + luteolin groups showed a typical morphology; with extensive dendritic arborisation climbing through the molecular layer toward the surface of the cortex, with axon originating at the opposite pole of the cell perikaryon, passing through the granular layer (where it becomes myelinated) towards the white matter, sending inhibitory efferent projections to the deep cerebellar nuclei. No differences in calbindin immunoreactivity were observed for other brain regions (dentate gyrus and CA1 pyramidal cells; data not shown).

3.7. Acetylcholinesterase activity

In this study, brain levels of acetylcholinesterase (AchE) activity was determined to evaluate the cholinergic mechanisms affecting locomotor activity in Co-exposed rats. Fig. 10 depicts the modulatory roles of luteolin and gallic acid on AchE activity in the brain of rats treated with $CoCl_2$. Administration of cobalt resulted in significant increase ($P < 0.05$) in AchE activity when compared to the control. However, co-administration with luteolin significantly reversed the Co-induced increase in AchE activity when compared with rats treated with $CoCl_2$ alone.

4. Discussion

The detection of high circulating levels of cobalt in patients with metal-on-metal hip prostheses has generated recent increased interest in cobalt toxicity to different body systems, including the nervous system. Neurological symptoms have long been described in patients with chronic occupational exposure to cobalt, as well as individuals

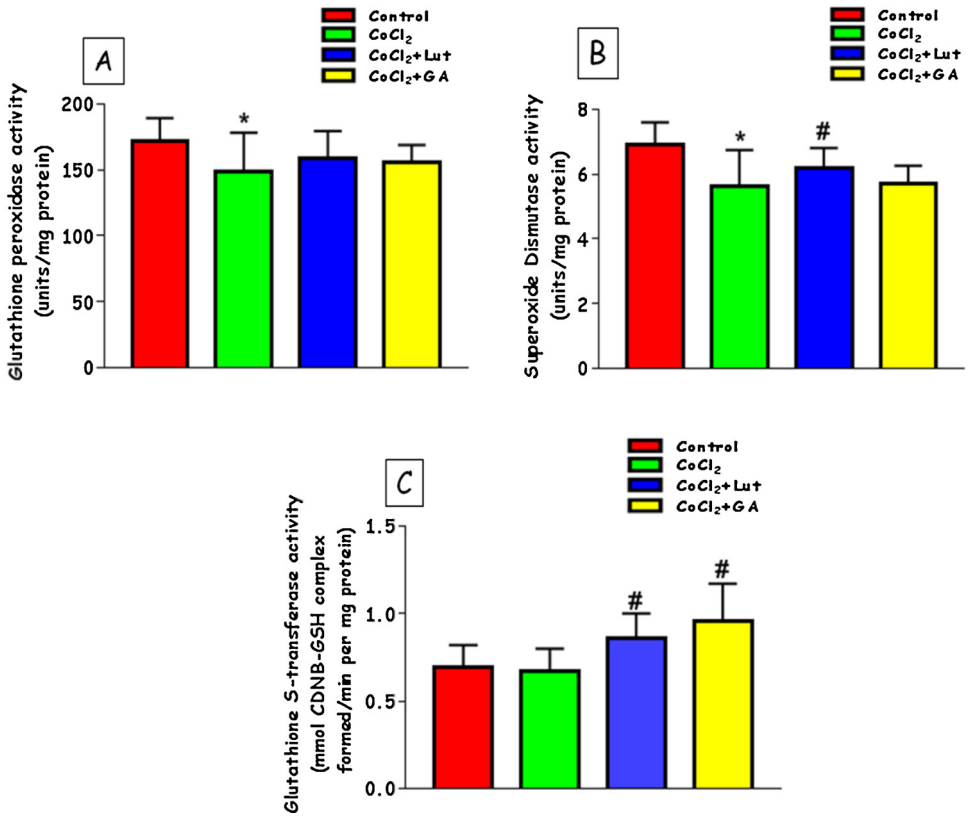

Fig. 6. Effect of Luteolin and Gallic acid on antioxidant enzymes in brain of rats exposed to Cobalt chloride. Values are expressed as mean ± standard deviation. * Significantly different from control, # significantly different from $CoCl_2$ only group.

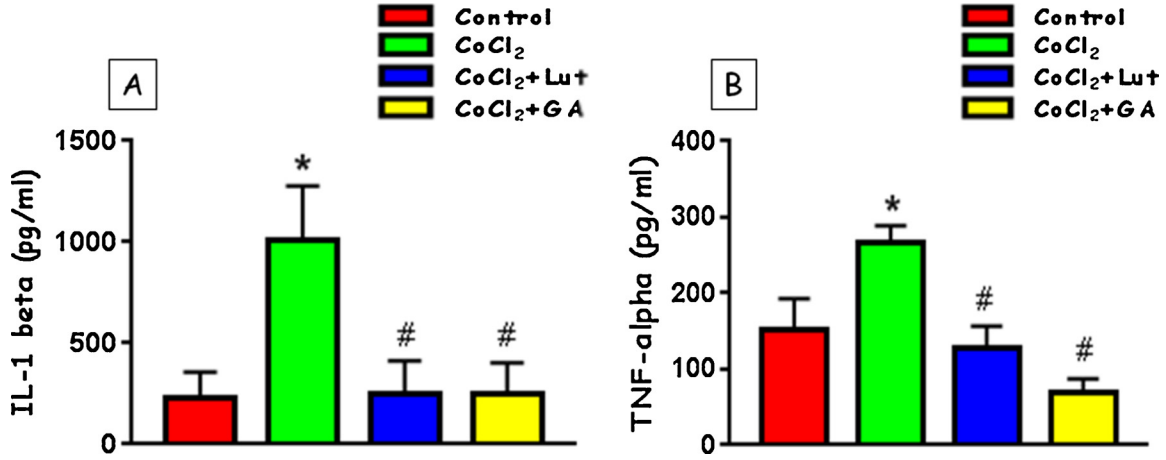

Fig. 7. Effect of Luteolin and Gallic acid on serum inflammatory cytokines in rats exposed to Cobalt chloride. Values are expressed as mean ± standard deviation. * Significantly different from control, # significantly different from $CoCl_2$ only group.

undergoing long-term treatment of anaemia with cobalt chloride (Catalani et al., 2012). However, very little information exists on the mechanism(s) of its neurotoxicity. The present study investigated various toxicity end-points in rats exposed to Cobalt chloride as well as the possible mechanisms involved in reversal of cobalt-induced neurotoxicity by two phenolic compounds, Luteolin and Gallic acid. Indeed, findings from this study showed that $CoCl_2$ (150 mg/kg) induced considerable changes in neuro-behavioural, oxidative, inflammatory, cholinergic responses in rats exposed for 7 days. In addition, this study demonstrated noticeable alterations in the motor-co-ordination centre of the central nervous system induced by cobalt administration.

The hanging wire test is a simple test that evaluates grip strength, balance and endurance. Administration of $CoCl_2$ caused sensory-motor impairment in the forelimb and significantly reduced the hanging ability of the rats. Co-treatment with luteolin, however, was able to restore motor coordination in the forelimb as suggested by the increased duration in latency to fall. Nevertheless, $CoCl_2$ administration did not interfere significantly with spatial learning and memory during the acquisition trail of the Morris water maze when compared to $CoCl_2$ + luteolin and control groups. The time required for spatial acquisition was, however, increased as depicted by longer escape latency during the acquisition trial depicting an extended time was required for learning in the $CoCl_2$ group.

The present result is in congruence with the loss of spatial learning reported by Jordan et al. (1990) following Co exposure in metal workers; however the result is in contrast with their report of

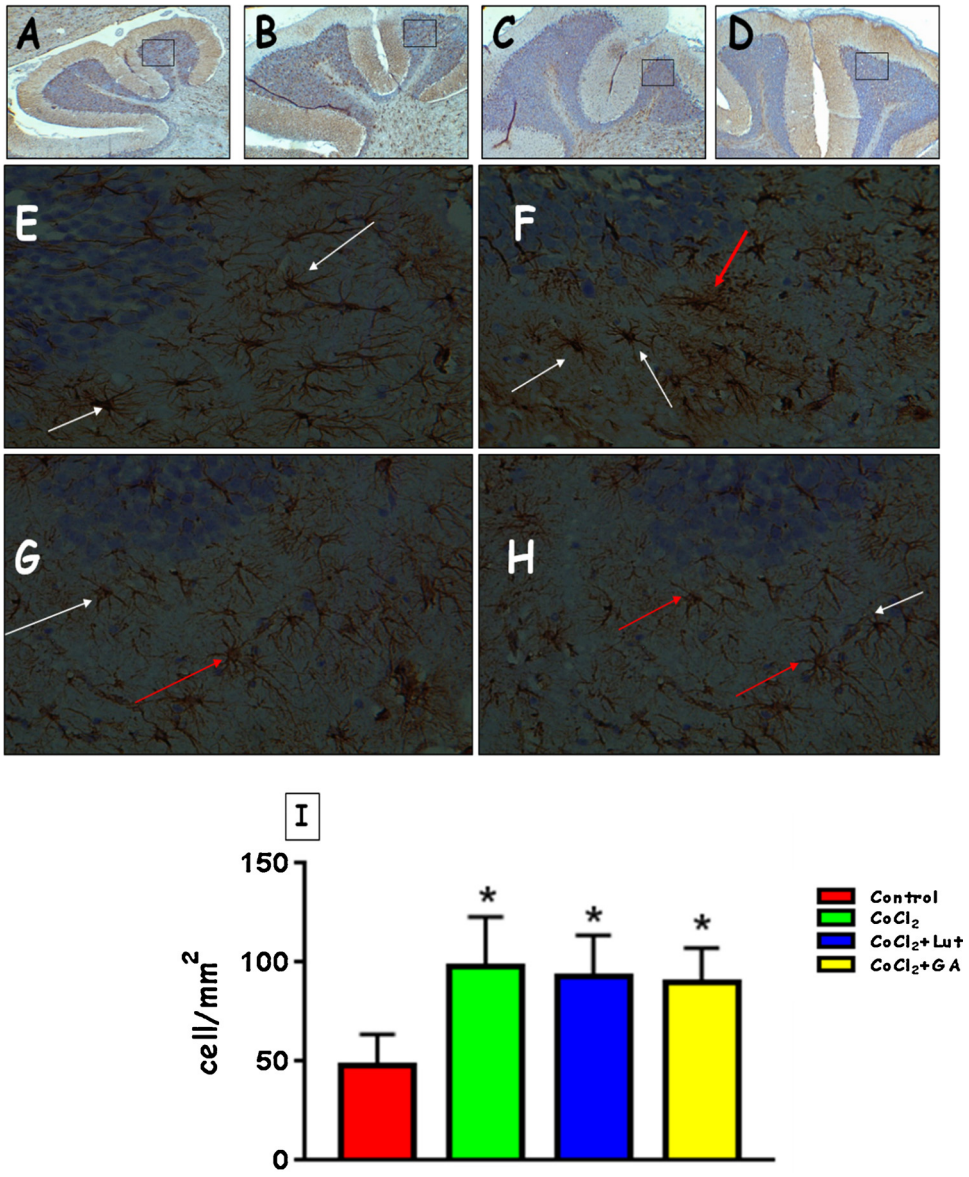

Fig. 8. Effect of cobalt chloride on the distribution of GFAP-positive astrocytes and GFAP cell count in the cerebellum. E, F, G and H are higher magnifications of boxed areas in A, B, C and D. Scale Bars in A, B, C and D = 200 μm Scale Bars in E, F, G and H = 50 μm. The quantification of GFAP-positive astrocyte cell number is shown in I. White arrows indicate GFAP-positive astrocytes. Note the few reactive astrocytes (i.e. swollen and ramified, in red arrows) in the $CoCl_2$, $CoCl_2$ + luteolin, $CoCl_2$ + gallic acid groups (F, G and H). (For interpretation of the references to colour in this figure legend, the reader is referred to the web version of this article.)

considerable impaired attention and memory loss. The differences in results may be attributed to the difference in species, dose, route and duration of exposure. It could be considered that the dose of the $CoCl_2$ used as well as the duration of its administration in the present study may not be enough to induce significant memory loss in rats. Administration of luteolin nevertheless restored delayed learning abilities to values comparable to the control group.

The Open Field test (OFT) is a simple method to assess motor function, normal exploratory, locomotor activity and anxiety in rodents (Prut and Belzung, 2003). In this study, the motor activity and exploratory behaviours of rats were characteristically affected by exposure to $CoCl_2$ as depicted by reduction in grid crosses as well as increased freezing and centre square duration. Increased stretched-attend posture (SAP) and faecal boli have been associated with anxiety (Shabani et al., 2012) in the OFT. The increased stretched attend posture reflects anxiety (Adebiyi et al., 2018) in the $CoCl_2$ group suggesting the possibility that luteolin may possess anxiolytic action as seen in its ability to reduce SAP to values comparable to control. In addition, its anxiolytic activity improved exploration and locomotion in rats.

The induction of oxidative stress is widely accepted as an important mechanism of cobalt toxicity (Catelas et al., 2005; Franco et al., 2009). The brain is highly susceptible to oxidative damage because of its high oxygen consumption (the brain consumes about 20% of the blood's oxygen), the terminally-differentiated nature of neurons and its relatively low activity of antioxidant enzymes (Dringen et al., 2000). The membranes of neurons are also rich in polyunsaturated fatty acids which are very prone to attack by ROS, leading to alterations in neuronal integrity and function (Mates, 2001). The results of the present study suggests that cobalt neurotoxicity was mediated, to some extent, by oxidative mechanisms including an overproduction of H_2O_2 and MDA, as well as down-regulation of key antioxidant enzymes including GPx, SOD and GST. Previous studies by Garoui et al (2013) lends support to the findings from this study as they also observed elevated levels of MDA and H_2O_2, along with reduction in GSH, GPx and SOD in the cerebrum and cerebellum of suckling pups with maternal exposure to cobalt. However, luteolin treatment effectively mediated the

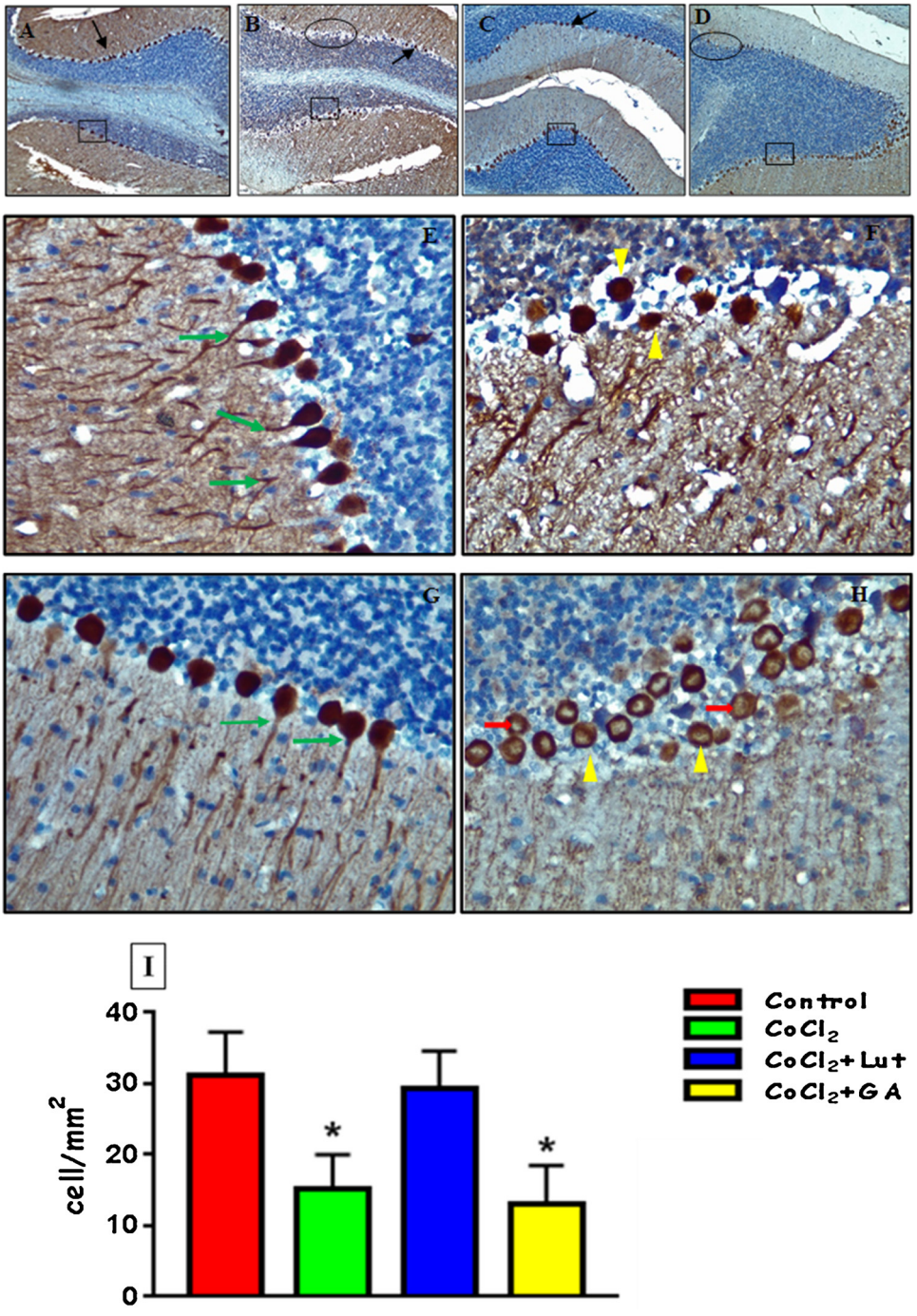

Fig. 9. Effect of cobalt on the distribution of calbindin-positive Purkinje cell (PC) and cell count in the cerebellum. E, F, G and H are higher magnification of boxed area in A, B, C and D. Scale bars in A, B, C and D = 200 μm, Scale bars in E, F, G and H = 50 μm. calbindin D-28k positive Purkinje cells conspicuously lined the cerebellum of control and $CoCl_2$ + luteolin rats (Fig. 9A, C) showing diffuse localization in PC cell bodies, apical dendrites, and their terminal arborizations in the molecular layer, as well as the predominantly infraganglionic plexus of PC axons transversing the internal granule layer (green arrows). In the $CoCl_2$ and $CoCl_2$ + Gallic acid rats calbindin D-28k loss of immunoreactivity (circle) were clearly observed with disorientation of cell bodies (yellow arrows, Figs. 9F and H). note the diminished staining of Purkinje cells in the $CoCl_2$ + Gallic acid (red arrows in Figs. 9H). The quantification of calbindin D-28k positive Purkinje cell number is shown in I. (For interpretation of the references to colour in this figure legend, the reader is referred to the web version of this article.)

restoration of Co-induced oxidative stress causing increased activities of GPx, SOD and GST, with concomitant reduction in H_2O_2 and MDA. These findings support reported antioxidant properties of luteolin (Lien et al., 1999).

Recent advances in the understanding of metal neurotoxicity have implicated microglia activation in the pathogenesis of neurological diseases. Studies have suggested a neuronal injury is often potentiated by metal-induced activation of microglia with subsequent release of inflammatory mediators (cytokines and chemokines) and nitric oxide (Mou et al., 2012). In the present study, cobalt exposure produced marked increases in the serum levels of the pro-inflammatory cytokines, TNFα and IL-1β, along with elevated levels of NO in the brain tissues. These findings are consistent with those of Mou et al (2012), who reported that high levels of Co caused up-regulation of the iNOS mRNA and protein in N9 cells and primary mouse microglia, leading to increased production of NO. These authors also reported concentration- and time-dependent increases in TNFα and IL-6 in the same cells. Treatment with both luteolin and gallic acid produced marked reversal of the pro-inflammatory effects of Co exposure lending support to previous literature citing the anti-inflammatory effects of these phenolic compounds (Xagorari et al., 2001).

Results of the current study showed that $CoCl_2$ have some destructive effects on motor co-ordinating region in central nervous system thus we, investigated the expression of astrocyte and Purkinje neurons in the brain. The Glial Fibrillary Acidic Protein (GFAP) is the major protein of glia intermediate filaments and is most commonly used as a marker for astroglial cells. Changes in astrocyte functionality are becoming recognized in increasing number of disease conditions (Seifert

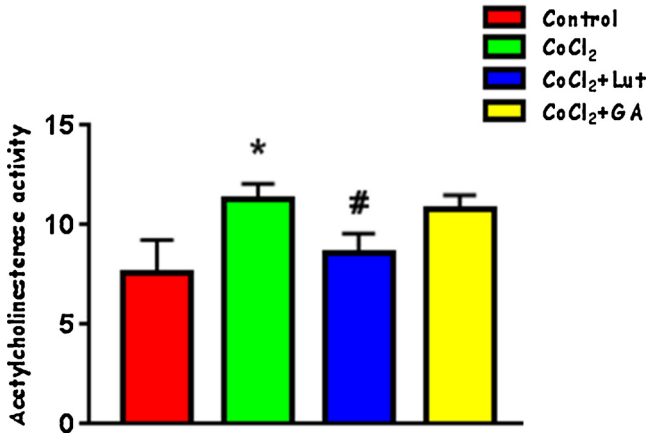

Fig. 10. Effect of Luteolin and Gallic acid on Acetylcholinesterase activity in rats exposed to Cobalt chloride. Values are expressed as mean ± standard deviation. * Significantly different from control, # significantly different from $CoCl_2$ only group.

et al., 2006), and the probable involvement of glia cells in neuronal plasticity and higher brain functions has been documented (Allaman et al., 2011). Astrocytes commonly undergo a dramatic transformation referred to as reactive astrocytosis or astrogliosis, which is perhaps the most prominent cellular response to diverse form of CNS injury. In line with previous study related to metal neurotoxicity we observed reactive astrogliosis in rat brain. GFAP immunostaining, clearly showed reactive astroglia in the cerebellum after $CoCl_2$ exposure. The activated astrocytes typically exhibit cytoplasmic hypertrophy, more numerous cytoplasmic processes which are longer and thicker in all the $CoCl_2$ exposed groups even after treatment with either luteolin or gallic acid. The upregulation of GFAP observed in our study was further quantified and suggested that the reactive astrogliosis is a physiological response to the exposure of the brain to this heavy metal.

The cerebellum is important for controlling and fine-tuning movements (Raymond et al., 1996: Mauk, 1997). The cerebellum receives multimodal inputs, via the pons, from numerous cortical (Middleton and Strick, 2001) regions and sends projections, via the thalamus, to several neocortical areas (Schmahmann, 2001) which are involved in a variety of cognitive functions that may be pertinent to Co neurotoxicity. The Purkinje cells (PCs) are indispensable for cerebellar function and their degeneration have been demonstrated to cause loss of muscle tone and impairment in locomotion (Lalonde and Strazielle, 2007). Variations in the calbindin D-28k (calbindin), a calcium-binding protein from cerebellar Purkinje cells have been associated with deficits of motor coordination and sensory processing (Barski et al., 2003). The absence of calbindin from this neuron, which exclusively provides an output from the cerebellar cortex, results in deficits in motor coordination/strength of the forelimb. The GABAergic axons of the PCs that form synapses on deep cerebellar nuclei neurons is also depleted as a result of PC degeneration by $CoCl_2$. The loss of GABAergic axons, severe depletion and disorganization of the Purkinje cells elucidates the neurobehavioral deficits and observed motor discordination seen in the $CoCl_2$ group and this degeneration could not be arrested by co-administration of gallic acid. In divergence luteolin administration was able to maintain the structural integrity of the Purkinje cells deeply correlating with maintenance of motor coordination in the behavioural tests.

The cerebellum is required for adaptation of automated compound movements to novel environments suggesting, therefore, that this function is particularly disturbed in $CoCl_2$ as well as $CoCl_2$ + gallic acid rats as seen in the open field test. These results, relating impaired motor coordination and reduced locomotion in the hanging wire and open field tests respectively to pathologies in the Purkinje cells of the cerebellum are remarkable because it may represent one of the major cellular correlates to the behavioural data.

Acetylcholinesterase (AchE) activity is a good indicator of the efficiency of cholinergic transmission. The enzyme mediates the degradation of acetylcholine (Ach) in the synaptic cleft. An increase in AchE activity, therefore, correlates with a reduction in Ach levels, reduced cholinergic transmission and consequent impairment of locomotor and exploratory activities. In the present study, the brain of rats exposed to Co presented with markedly increased AchE activity, compared to the control and control + luteolin groups. This finding is in agreement with much older reports by Giovannini et al (1978) who reported increase in erythrocyte AchE after exposure of rabbits to cobalt. Cobalt is known to induce blockade of synaptic transmission via pre-synaptic blockade of calcium channels, also resulting in decreased exploratory behaviour (Czarnota et al., 1998). The stimulation of AchE activity, therefore, represents another important mechanism of Co-induced impairment of neuro-behavioural activities. The effectiveness of Luteolin in restoring AchE activity to control levels suggests that it may likely exert better enhancement of cholinergic activity compared to gallic acid. It should be pointed out that the restoration of AchE activity by luteolin may explain, at least in part, the improved locomotor and exploratory activities observed in the rats administered this flavonoid.

In summary, we have provided evidence to support a model of how brain neuron and astrocyte signals underlie the mechanisms of cobalt poisoning. We showed that cobalt elicited disturbance in motor co-ordination and diminished learning. The reactive astrogliosis observed in an acute $CoCl_2$ toxicity may play a role as first line defence in protecting the central nervous system. The damage to Purkinje neurons in the present study further gives credence to the interaction between neurons and astrocytes under pathological conditions. In this study, a pathway for luteolin in protecting against $CoCl_2$ is probably the inhibition of damage to Purkinje neurons in the cerebellum.The maintenance of Purkinje cell integrity was probably mediated by the antioxidant and anti-inflammatory exerted by the flavonoids, luteolin and gallic acid.

Declaration of Competing Interest

The authors declare that they have no known competing financial interests or personal relationships that could have appeared to influence the work reported in this paper.

Acknowledgements

The authors are grateful to Dr A.A. Oyagbemi for graciously donating some compounds used in this study; Dr. AI Adebiyi for his assistance with the ELISA experiments and Dr. KO Adigun for helping with some of the experiments. This research did not receive any specific grant from funding agencies in the public, commercial, or not-for-profit sectors.

Appendix A. Supplementary data

Supplementary material related to this article can be found, in the online version, at doi:https://doi.org/10.1016/j.neuro.2019.07.005.

References

Aartsma-Rus, A., van Putten, M., 2014. Assessing functional performance in the Mdx mouse model. J Vis Exp. 85. https://doi.org/10.3791/51303.

Adebiyi, O.E., Olopade, J.O., Olayemi, F.O., 2018. Sodium metavanadate induced cognitive decline, behavioral impairments, oxidative stress and down regulation of MBP in mice hippocampus: ameliorative roles of β-spinasterol and stigmasterol. Brain Behav. https://doi.org/10.1002/brb3.1014.

Akinrinde, A.S., Omobowale, O.O., Oyagbemi, A., Asenuga, E., Ajibade, T., 2016a. Protective effects of Kolaviron and gallic acid against cobalt chloride-induced cardiorenal dysfunction via suppression of oxidative stress and activation of the ERK signalling pathway. Can. J. Physiol. Pharmacol. 94, 1276–1284. https://doi.org/10.1139/cjpp-2016-0197.

Akinrinde, A.S., Oyagbemi, A.A., Omobowale, T.O., Asenuga, E.R., Ajibade, T.O., 2016b. Alterations in blood pressure, antioxidant status and caspase 8 expression in cobalt-chloride induced cardio-renal dysfunction are reversed by Ocimum gratissimum and

gallic acid in Wistar rats. J. Trace Elem. Med. Biol. 36, 27–37. https://doi.org/10.1016/j.jtemb.2016.03.015.
Allaman, I., Be´langer, M., Magistretti, P.J., 2011. Astrocyte– neuron metabolic relationships: for better and for worse. Trends Neurosci. 34 (2), 76–87. https://doi.org/10.1016/j.tins.2010.12.001.
Awoyemi, O.V., Okotie, U.J., Oyagbemi, A.A., Omobowale, T.O., Asenuga, E.R., Ola-Davies, O.E., Ogunpolu, B.S., 2017. Cobalt chloride exposure dose-dependently induced hepatotoxicity through enhancement of cyclooxygenase-2 (COX-2)/B-cell associated protein X (BAX) signaling and genotoxicity in Wistar rats. Environ. Toxicol. 32 (7), 1899–1907. https://doi.org/10.1002/tox.22412.
Barski, J.J., Hartmann, J., Rose, C.R., Hoebeek, F., Mörl, K., Noll-Hussong, M., De Zeeuw, C.I., Konnerth, A., Meyer, M., 2003. Calbindin in cerebellar Purkinje cells Is a critical determinant of the precision of motor coordination. J. Neurosci. 23 (8), 3469–3477.
Beutler, E.O., Duron, B., Kelly, M., 1963. Improved method for the determination of blood glutathione. J. Lab Clin. Med. 61, 882–888.
Brown, R., Corey, S., Moore, A., 1999. Differences in measures of exploration and fear in MHC-congenic C57BL/6J and B6-H-2K mice. Behav Gen. 29 (4), 263–271. https://doi.org/10.1023/A:1021694307672.
Catalani, S., Rizzetti, M.C., Padovani, A., Apostoli, P., 2012. Neurotoxicity of cobalt. Hum. Exp. Toxicol. 31 (5), 421–437. https://doi.org/10.1177/0960327111414280.
Catelas, I., Petit, A., Vali, H., Pragiskatos, C., Meilleur, R., Zukov, D.J., et al., 2005. Quantitative analysis of macrophage apoptosis vs necrosis induced by cobalt and chromium ions in vitro. Biomaterials 26, 2441–2453. https://doi.org/10.1016/j.biomaterials.2004.08.004.
Cheyns, K., Banza, Lubaba, Nkulu, C., Ngombe, L.K., Asosa, J.N., Haufroid, V., De Putter, T., et al., 2014. Pathways of human exposure to cobalt in Katanga, a mining area of the D.R. Congo. Sci. Total Environ. 490, 313–321. https://doi.org/10.1016/j.scitotenv.2014.05.014.
Czarnota, M., Whitman, D., Berman, R., 1998. Activity and passive avoidance learning in cobalt-injected rats. Int. J. Neurosci. 93, 29–33.
Deng, C., Gao, C., Tian, X., Chao, B., Wang, F., Zhang, Y., Zou, J., Liu, D., 2017. Pharmacokinetics, tissue distribution and excretion of luteolin and its major metabolites in rats: metabolites predominate in blood, tissues and are mainly excreted in bile. J. Funct. Foods 35, 332–340.
Dringen, R., Gutterer, J.M., Hirrlinger, J., 2000. Glutathione metabolism in brain metabolic interaction between astrocytes and neurons in the defense against reactive oxygen species. Eur. J. Biochem. 267, 4912–4916.
Franco, R., Sanchez-Olea, R., Reyes-Reyes, E.M., Panayiotidis, M.I., 2009. Environmental toxicity, oxidative stress and apoptosis: ménage a trios. Mutat. Res. Genet. Toxicol. Environ. Mutagen. 674, 3–22. https://doi.org/10.1016/j.mrgentox.2008.11.012.
Garoui, E., Amara, I.B., Driss, D., Elwej, A., Chaabouni, S.E., Boudawara, T., 2013. Effects of cobalt on membrane ATPases, oxidant and antioxidant values in the cerebrum and cerebellum of suckling rats. Biol. Trace Elem. Res. 154 (3), 387–395. https://doi.org/10.1007/s12011-013-9746-0.
Giovannini, E., Principato, G.B., Ambrosini, M.V., Grassi, G.G., Dell' Agata, M., 1978. Erythrocyte acetylcholinesterase activity changes in the early stages of anemic and hypobaric hypoxia or after $CoCl_2$ treatment in rabbits. Acta Haemat. 60, 21–28.
Golchin, L., Golchin, L., Vahidi, A.A., Shabani, M., 2013. Hippocampus and cerebellum function following imipenem treatment in male and female rats: evaluation of sex differences during developmental stage. Pak. J. Biol. Sci. 16 (4), 151–159.
Gornal, A.G., Bardawill, J.C., David, M.M., 1949. Determination of serum proteins by means of Biuret reaction. J. Biol. Chem. 177, 751–766.
Habig, W.H., Pabst, M.J., Jacoby, W.B., 1974. Glutathione-S-transferase activity: the enzymic step in mercapturic acid formation. J. Biol. Chem. 249, 130–139.
Jalayeri-Darbandi, Z., Rajabzadeh, M.A., Hosseini, M., Beheshti, F., Ebrahimzadeh-Bideskan, A., 2018. The effect of methamphetamine exposure during pregnancy and lactation on hippocampal doublecortin expression, learning and memory of rat offspring. Anat. Sci. Int. 93 (3), 351–363. https://doi.org/10.1007/s12565-017-0419-5.
Jensen, E.C., 2013. Quantitative analysis of histological staining and fluorescence using ImageJ AR insights. Anatom. Record 296, 378–381. https://doi.org/10.1002/ar.22641.
Jiang, L., Li, H., Zhao, N., 2017. Thymoquinone protects against cobalt chloride-induced neurtoxicity in Nrf 2/GCL-regulated glutathione homeostasis. J. Biol. Regul Homeost. Agents. 31 (4), 843–853.
Jordan, C., Whitman, R.D., Harbut, M., 1990. Memory deficits in workers suffering from hard metal disease. Toxicol. Lett. 54, 241–243.
Keegan, G.M., Learmonth, I.D., Case, C.P., 2019. Orthopaedic metals and their potential toxicity in the arthroplasty patient: a review of current knowledge and future strategies. J. Bone Joint Surg. Br. 89, 567–573.
Kubrak, O.I., Husak, V.V., Rovenko, B.M., Storey, J.M., Storey, K.B., Lushchak, V.I., 2011. Cobalt-induced oxidative stress in brain, liver and kidney of goldfish Carassius auratus. Chemosphere 85 (6), 983–989. https://doi.org/10.1302/0301-620X.89B5.18903.
Lalonde, R., Strazielle, C., 2007. Spontaneous and induced mouse mutations with cerebellar dysfunctions: behavior and neurochemistry. Brain Res. 6, 51–74. https://doi.org/10.1016/j.brainres.2006.01.031.
Li, R.W., Klein, S.A., Levi, D.M., 2008. Prolonged perceptual learning of positional acuity in adult amblyopia: perceptual template retuning dynamics. J. Neurosci. 28, 14223–14229 https://dx.doi.org/10.1523%2FJNEUROSCI.4812-10.2010.
Lien, E.J., Ren, S., Bui, H.H., Wang, R., 1999. Quantitative structure-activity relationship analysis of phenolic antioxidants. Free Radic. Biol. Med. 26, 285–294.
Lin, Y., Shi, R., Wang, X., Shen, H.-M., 2008. Luteolin, a flavonoid with potentials for cancer prevention and therapy. Curr. Drug. Ther. 8 (7), 634–646.
Lu, H., Chen, Y., Sun, X.-B., Tong, B., Fan, X.-H., 2015. Effects of luteolin on retinal oxidative stress and inflammation in diabetes. RSC Adv. 5, 4898–4904. https://doi.org/10.1039/C4RA10756J.
Mansouri, M.T., Farbood, Y., Sameri, M.J., Sarkaki, A., Naghizadeh, B., Rafeirad, M., 2013. Neuroprotective effects of oral gallic acid against oxidative stress induced by 6-hydroxydopamine in rats. Food Chem. 136 (2-3), 1028–1033.
Mao, X., Wong, A., Crawford, R.W., 2011. Cobalt toxicity — an emerging clinical problem in patients with metal-on-metal hip prostheses? Med. J. Aust. 194 (12), 649–651.
Mates, J.M., 2001. Effects of antioxidant enzymes in the molecular control of reactive oxygen species. Toxicology 163 (2-3), 219.
Mauk, M.D., 1997. Roles of cerebellar cortex and nuclei in motor learning: contradictions or clues. Neuron. 18 (3), 343–346.
Middleton, F.A., Strick, P.L., 2001. Cerebellar projections to the prefrontal cortex in the primate. J Neurosci. 21, 700–712.
Misra, H.P., Fridovich, I., 1972. The role of superoxide anion in the autooxidation of epinephrine and a simple assay for superoxide dismutase. J. Biol. Chem. 247, 3170–3175.
Mobasheri, A., Proudman, C.J., 2015. Cobalt chloride doping in racehorses: concerns over a potentially lethal practice. Vet. J. 205, 335–338. https://doi.org/10.1016/j.tvjl.2015.04.005.
Mohamed, A.A.R., Metwally, M.M.M., Khalil, S.R., et al., 2019. *Moringa oleifera* extract attenuates the $CoCl_2$ induced hypoxia of rat's brain: expression pattern of HIF-1 < alpha > , NF-kB, MAO and EPO. Biomed. Pharmacother. 109, 1688–1697.
Morris, R., 1984. Developments of a water-maze procedure for studying spatial learning in the rat. J. Neurosci. Methods 11, 47–60.
Mou, Y.H., Yang, J.Y., Cui, N., Wang, J.M., Hou, Y., Song, S., Wu, C.F., 2012. Effects of cobalt chloride on nitric oxide and cytokines/chemokines production in microglia. Int. Immunopharmacol. 13 (1), 120–125.
Olaleye, S.B., Adaramoye, O.A., Erigbali, P.P., Adeniyi, O.S., 2007. Lead exposure increases oxidative stress in the gastric mucosa of HCl/ethanol-exposed rats. World J. Gastroenterol. 13, 5121–5126. https://doi.org/10.3748/wjg.v13.i38.5121.
Olivieri, J., Hess, C., Savaskan, E., Ly, C., Meier, F., Baysang, G., Muller-Spahn, F., et al., 2001. Melatonin protects SHSY5Y neuroblastoma cells from cobalt-induced oxidative stress, neurotoxicity and increased beta-amyloid secretion. J. Pineal Res. 31, 320–325. https://doi.org/10.1034/j.1600-079X.2001.310406.x.
Oyagbemi, A.A., Omobowale, T.O., Akinrinde, A.S., Saba, A.B., Ogunpolu, B.S., Daramola, O., 2015. Lack of reversal of oxidative damage in renal tissues of lead acetate treated rats. Environ. Toxicol. 30 (11), 1235–1243. https://doi.org/10.1002/tox.21994.
Oyagbemi, A.A., Afolabi, J.M., Ogunpolu, B.S., Falayi, O.O., Saba, A.B., Adedapo, A.A., Yakubu, M.A., 2018. Luteolin-mediated Kim-1/NFκB/Nrf2 signaling pathways protects sodium fluoride-induced hypertension and cardiovascular complications. Biofactors. 44 (6), 518–531.
PHS (PUBLIC HEALTH SERVICE), 1996. Public Health Service Policy on Humane Care and the Use of Laboratory Animals. US Department of Health and Humane Services, Washington, DC, pp. 99–158.
Prut, L., Belzung, C., 2003. The open field as a paradigm to measure the effects of drugs on anxiety-like behaviors: a review. Eur. J. Pharmacol. 463 (1–3), 3–33.
Rajabzadeh, A., Bideskan, A.E., Fazel, A., Sankian, M., Rafatpanah, H., Haghir, H., 2012. The effect of PTZ-induced epileptic seizures on hippocampal expression of PSA-NCAM in offspring born to kindled rats. J. Biomed. Sci. 19, 56. https://doi.org/10.1186/1423-0127-19-56.
Raymond, J.L., Lisberger, S.G., Mauk, M.D., 1996. The cerebellum: a neuronal learning machine? Science 272, 1126–1131.
Rotruck, J.T., Pope, A.L., Ganther, H.E., Swanson, A.B., Hafeman, D.G., Hoekstra, W., 1973. Selenium: biochemical role as a component of glutathione peroxidase. Science 179, 588–590.
Schmahmann, J.D., 2001. The cerebrocerebellar system: anatomic substrates of the cerebellar contribution to cognition and emotion. Int. Rev. Psychiatry 13, 247–260. https://doi.org/10.1080/09540260120082092.
Seifert, G., Schilling, K., Steinhauser, C., 2006. Astrocyte dysfunction in neurological disorders: a molecular perspective. Nat. Rev. Neurosci. 7, 194–206. https://doi.org/10.1038/nrn1870.
Shabani, M., Larizadeh, M.H., Parsania, S., Shekaari, M.A., Shahrokhi, N., 2012. Profound destructive effects of adolescent exposure to vincristine accompanied with some sex differences in motor and memory performance. Can. J. Physiol. Pharmacol. 90, 379–386. https://doi.org/10.1139/y11-132.
Speijers, G.J.A., Krajnc, E.I., Berkvens, J.M., van Logten, M.J., 1982. Acute oral toxicity of inorganic cobalt compounds in rats. Food Chem Toxicol. 20 (3), 311–314.
Tan, C., Gao, M., Xu, W., Yang, X., Zhu, X., Du, G., 2009. Protective effects of Salidroside on endothelial cell apoptosis induced by cobalt chloride. Biol. Pharm. Bull. 32 (8), 1359–1363.
Tvermoes, B.E., Finley, B.L., Unice, K.M., Otani, J.M., Paustenbach, D.J., Galbraith, D.A., 2013. Cobalt whole blood concentrations in healthy adult male volunteers following two-weeks of ingesting cobalt supplement. Food Chem. Toxicol. 53, 432–439. https://doi.org/10.1016/j.fct.2012.11.033.
Varga, D., Heredi, J., Kanvasi, Z., Ruszka, M., Kis, Z., Ono, E., Iwamori, N., Iwamori, T., Takakuwa, H., Vecsei, L., Toldi, J., Gellert, L., 2015. Systemic L-Kynurenine sulfate administration disrupts object recognition memory, alters open field behavior and decreases c-Fos immunopositivity in C57BI/6 mice. Front. Behav. Neurosci. 9, 14–24.
Varshney, R., Kale, R.K., 1990. Effect of calmodulin antagonists on radiation induced lipid peroxidation in microsomes. Int. J. Biol. 158, 733–741.
Vengellur, A., LaPres, J.J., 2004. The role of hypoxia-inducible factor alpha incobalt-chloride-induced cell death in mouse embryonic fibroblasts. Toxicol.Sci. 82, 638–646. https://doi.org/10.1093/toxsci/kfh278.
Wolff, S.F., 1994. Ferrous ion oxidation in the presence of ferric ion indicator xylenol orange for measurement of hydrogen peroxides. Methods Enzymol. 233, 182–189.
Xagorari, A., Papapetropoulos, A., Mauromatis, A., Economou, M., Fotsis, T., Roussos, C., 2001. Luteolin inhibits an endotoxin-stimulated phosphorylation cascade and

proinflammatory cytokine production in macrophages. J. Pharmacol. Exp. Ther. 296, 181–187.
Zhang, Y.-C., Gan, F.F., Shelar, S.B., Ng, K.-Y., Chew, E.-H., 2013. Antioxidant and Nrf2 inducing activities of luteolin, a flavonoid constituent in *Ixeris sonchifolia* Hance, provide neuroprotective effects against ischemia-induced cellular injury. Food Chem. Toxicol. 59, 272–280.
Zhao, C., Deng, W., Gage, H., 2008. Mechanisms and functional implications of adult neurogenesis. Cell. 132 (4), 645–666. https://doi.org/10.1016/j.cell.2008.01.033.
Zheng, F., Luo, Z., Zheng, C., et al., 2019. Comparison of the neurotoxicity associated with cobalt nanoparticles and cobalt chloride in Wistar rats. Toxicol. Appl. Pharmacol. 369, 90–99.